OPEN ACCESS

University of BRISTOL

Wang, H., Ramakrishnan, K. R., & Shankar, K. (2016). Experimental study of the medium velocity impact response of sandwich panels with different cores. *Materials and Design*, *99*, 68-82. https://doi.org/10.1016/j.matdes.2016.03.048

Peer reviewed version

License (if available):
CC BY-NC-ND

Link to published version (if available):
10.1016/j.matdes.2016.03.048

Link to publication record in Explore Bristol Research
PDF-document

This is the author accepted manuscript (AAM). The final published version (version of record) is available online via Elsevier at https://www.sciencedirect.com/science/article/abs/pii/S0264127516303239 . Please refer to any applicable terms of use of the publisher.

University of Bristol - Explore Bristol Research
General rights

This document is made available in accordance with publisher policies. Please cite only the published version using the reference above. Full terms of use are available:
http://www.bristol.ac.uk/red/research-policy/pure/user-guides/ebr-terms/

Experimental study of the medium velocity impact response of sandwich panels with different cores

Hongxu Wang, Karthik Ram Ramakrishnan*, Krishna Shankar

School of Engineering and Information Technology, University of New South Wales Canberra, ACT 2600, Australia

*Corresponding author. Tel.: +61 2 62688258

E-mail address: Karthik.ramakrishnan@adfa.edu.au

Abstract:

The impact response of sandwich panels is not only dependent on the facesheet but also on the core material. The choice of the core has a strong effect on the strength and durability of the structure. This paper compares the dynamic response of sandwich panels with different core materials when subjected to medium velocity impacts. The sandwich panels were made of aluminium facesheets with five different cores, viz., low density balsa wood, high density balsa wood, cork, polypropylene honeycomb, and polystyrene foam. All the specimens were impacted by a 384.4 g instrumented projectile with a hemispherical steel head at three impact energies of 43, 85 and 120 J. An accelerometer attached to the projectile and a high speed camera were used to collect data and record the impact process. 3D scanning technique was used to measure the deformation of front and back faces after impact. The impact properties of the sandwich panels with the five different cores were compared in terms of contact force, energy absorption, depth of indentation, overall bending deflection, etc. Post-mortem sectioning was also conducted to examine the impact

induced failures such as facesheet rupture, crush of core material, and debonding between facesheet and core.

Keywords: core material; energy absorption; failure mechanism; impact; sandwich panel.

1. Introduction

The increasing effort to develop lightweight structures characterised by better mechanical performance has led to the development and employment of sandwich structures. A sandwich structure may be defined as a composite component featuring a lightweight core placed between two relatively thin high-strength facesheets or skins. The facesheets are designed to resist bending loads and are usually made of aluminium or fibre reinforced polymers. The core separates and stabilises the outer sheets against buckling under edgewise compression, torsion or bending and is usually made of woods, expanded metals, polymer and metal foams, and polymer and metal honeycombs [1]. An adhesive bonding between the facesheets and core ensures the load transfer between them. Sandwich structures are lightweight composite materials that have been widely used in numerous application fields such as aerospace, marine, automotive, and energy industries for their desirable properties like high specific bending stiffness, excellent thermal insulation, acoustic damping, etc. However, sandwich composite structures are susceptible to impact loading and may be subjected to different impacts such as tool drops, bird strikes, hail stones, and runway debris during the service life [2]. These impacts may cause significant damage, such as local core crushing and debonding of the facesheet from the core, which severely compromises the structural integrity of the sandwich panel [3]. The study on the behaviour of sandwich structures subjected to impact loading is usually accomplished by experimental testing [4-6]. The effects of impact variables

(such as impact velocity and energy, impactor shape and diameter) and sandwich construction parameters (core material and thickness, facesheet type) on the impact behaviour and resulting damage are the major concerns in many studies. According to Ozdemir et al. [7], the core material and thickness is one of the main factors determining the impact behaviour of sandwich structures and it was shown that the energy absorption capacity of sandwich composites increased with increasing core thickness.

The core materials are usually divided into four groups: balsa woods, corrugated sheets, honeycombs and cellular foams [8]. Aluminium honeycombs have been used in the aerospace industry but suffer from corrosion damage to the core from water ingress. According to Shipsha [8], though honeycomb cored sandwich structures offer the highest stiffness to weight ratio, many industrial applications prefer cellular foam cores such as polyvinyl chloride (PVC) foam because of their relative low cost, water resistance, and a possibility to use traditional manufacturing methods such as hand layup. Foam materials have a cellular structure with a three-dimensional array of cells and this microscopic cellular structure determines their superior performance as an energy absorbing material [9]. Another advantage of foam cores is the increased support surface for bonding with the facesheets [10]. Foams that are used as core materials for sandwich structures include polyurethane foams, phenolic foams, expanded and extruded polystyrene (EPS and XPS) foams and polymethacrylimide (PMI) foams [11]. Cantwell et al. [5] compared the impact response of sandwich structures with balsa wood and PVC foam cores for use in marine applications. Bernard and Lagace [12] studied the impact resistance of composite sandwich plates with graphite/epoxy facesheets and three different cores which were aluminium honeycomb, Nomex honeycomb and Rohacell foam using low energy impact tests. Atas and Sevim [13] compared the impact damage process of sandwich samples with PVC foam and balsa wood cores by cross-examining the load–deflection curves, energy profile diagrams, and damaged

specimens. Another popular type of core used for manufacturing sandwich panels is metallic foam. Mohan et al. [14] experimentally investigated the response of bare aluminium foam blocks and their sandwich panels with various tailored facesheets under a drop-weight impact loading; the results showed increase in foam thickness and the use of facesheet enhanced the impact energy absorption capacity. Rajaneesh et al. [15] compared the relative performance of sandwich plates consisting of aluminium alloy foam and PVC foam with aluminium facesheets under low velocity impact, and it was found that the contact radius was higher for a sandwich plate with a stronger foam for a given impact load. Hou et al. [16] conducted ballistic impact experiments on metallic sandwich panels with aluminium foam core, and it was revealed an approximate linear relationship between ballistic limit and relative core density. Moreover, the ballistic limit of the specimens with a thicker core had a more rapid increase with the relative density than their counterparts with thinner core.

The understanding of the impact phenomenon and the damage mechanisms are essential for developing improved materials [17]. The impact problem can be classified as low velocity impact by a large mass (like a dropped tool), which is simulated using a falling weight or a swinging pendulum, and medium/high velocity impact by a small mass (such as runway debris, small firearms, etc.), which is simulated with a gas gun or some other ballistic launchers [18]. It is generally accepted that low velocity impact are impacts at velocities below 10 m/s, medium velocity impact has velocities ranging from 10 to 50 m/s, and high velocity impact occurs in the 50 to 1000 m/s velocity range [18, 19]. While low velocity impact [14, 15, 20-23] and high velocity impact [4, 16, 24] response of sandwich panels are well represented in the literature, the response of sandwich panels subjected to medium velocity impacts has rarely been studied experimentally. In this paper, sandwich panels with aluminium facesheets and five different core materials are impacted at different energies

using a medium velocity gas gun and a comparison based on the force–displacement response and failure modes of the panels is presented.

2. Experimental methodology

2.1. Materials used

The sandwich panels tested in this study were manufactured of identical facesheets combined with five different core materials using a wet layup process. The material of the facesheet was Aluminium 2024-T3, and the core materials were Balsa wood of low density (LD) and high density (HD), Cork, Polypropylene (PP) honeycomb, and Polystyrene (PS) foam. It was found that the core height has a significant influence on the impact response of sandwich structures [7, 16, 25, 26], so the thicknesses of cores were kept nominally constant to eliminate the geometry effect on the bending stiffness, leaving only the effect of the material properties of the core as the variable. Table 1 summarises the properties of all the materials used: the thickness and density were measured directly while the Young's modulus, compressive strength, and shear strength were obtained from the manufacturer's data and published literature [27, 28]. The core materials were chosen as representative of the different types of cores used in sandwich construction. The balsa wood core supplied by Baltek is reported to have optimum physical properties due to its honeycomb-like cell structure obtained by cutting perpendicular to the grain direction. Toson et al. [29] reported that wood material such as balsa is of particular interest for application as a core material in sandwich panels because of its transversely isotropic behaviour, i.e., it is stiff and strong in the direction of the fibres (axial) and transversely compliant (in directions that are tangential and radial to it growth rings). The expanded polystyrene foam supplied by Polyfoam is a closed cell, thermoplastic, lightweight, and rigid cellular plastic material and is chosen for its

excellent energy absorbing and damping properties. Polypropylene honeycomb supplied by Polycore with cell size of 8 mm was chosen for sandwich core material with honeycomb construction. The natural honeycomb structure of the closed cells of cork core was chosen for its low density, high compressibility and excellent recovery characteristics.

Table 1. Material properties.

Material	Al 2024-T3	Balsa LD	Balsa HD	Cork	PS Foam	PP Honeycomb
Thickness (mm)	1.06	10.45	10.32	10.23	9.52	10.74
Density (kg/m^3)	2614.42	101.77	145.04	150.43	32.39	145.21
Young's Modulus (MPa)	73100	10~18	10~18	5.1	8~20	97
Compressive Strength (MPa)	483	2.5	2.5	0.3	0.3	2.2
Shear Strength (MPa)	283	9	9	5.9	4.5	19

The bonding surface of the aluminium facesheet must be free of any contaminants such as grease, oil, wax or mold release. The surface of facesheet was cleaned of oxide material and contaminant using abrasive sand paper and acetone. The facesheets were bonded on each side of the core material using the West System two-part epoxy resin, and the sandwich panel was placed in a vacuum bag to cure for 24 hours at room temperature. The cured sandwich panels were cut into 150 mm × 150 mm squares for impact test.

2.2. Impact testing

The medium velocity impact response of sandwich structures is typically tested using a gas gun [30]. A steel projectile with a hemispherical nose having a diameter of 20 mm, as shown in Fig. 1 (a), was used to impact the centre of sandwich panels perpendicularly. A piezoelectric accelerometer mounted within the projectile with flexible wires and connected to a National Instruments high-speed data acquisition system with a sampling rate of 100 kHz was employed to capture the uniaxial acceleration history of the projectile during impact. The wires were made to snap if the projectile rebound out of the reach of the wires. The recorded acceleration data was cleaned of spurious noise by a Butterworth low pass filter (cut-off frequency of 5000 Hz) and converted to force by multiplying it by the total mass of the projectile which was 384.4 g. A vertical gas gun, as shown in Fig. 1 (b), was employed to propel the projectile to three different velocities which were 15, 21, and 25 m/s resulting in impact energies of 43, 85, and 120 J. Only one sample of each type of sandwich panels was tested in the three initial velocity conditions. According to Cantwell and Morton [18], the impact test fixture should be designed to simulate the loading conditions to which a composite component is subject in operational service and then reproduce the failure modes and mechanisms likely to occur. The square sandwich specimen was clamped horizontally using two steel annular solids with an internal diameter of 135 mm, as seen in Fig. 1 (d). The top solid was removable while the bottom one was fixed on a rigid stand. Four bolts were tightened to a torque of 5 N·m in order to provide a consistent clamping condition from test to test. Similar circular fixtures were used to evaluate the low velocity impact response of sandwich panels [2, 31] and composite laminates [32, 33] under drop weight impact tests. A protective cage, as shown in Fig. 1 (c), was placed around the mounting stand in order to prevent the projectile ricocheting and hitting the surrounding equipment during the impact tests. Two sides of the cage were made of ply wood while the other two sides were covered using transparent Perspex in order to observe and record the impact process using a high

speed camera. The top side consisted of wire mesh and a rubber ‘rebound catcher’ (see Fig. 1 (e)) which allowed the projectile to pass through without any loss of velocity but not rebound out of the protective cage and collide with the shaft of the gas gun.

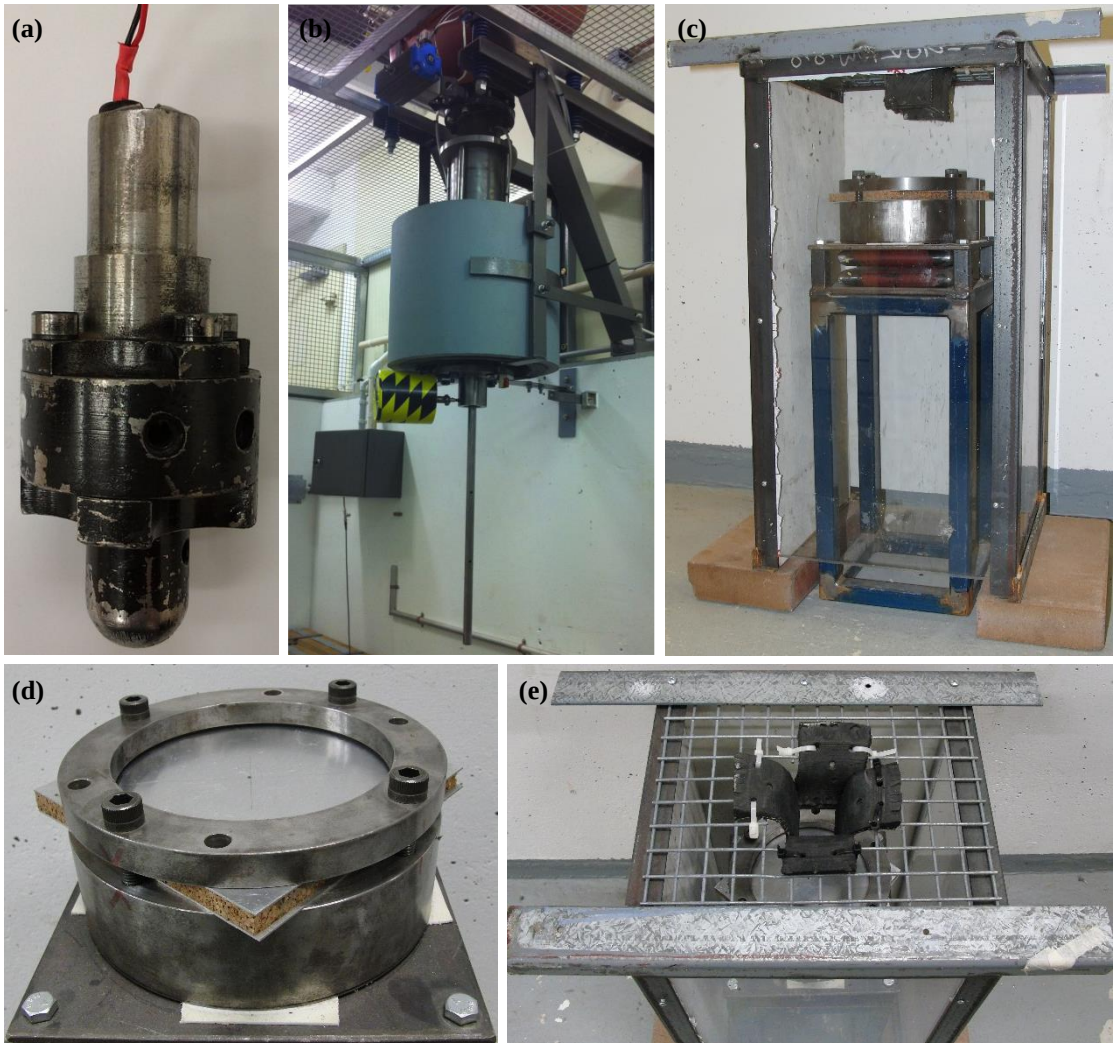

Fig. 1. Experimental setup: (a) instrumented projectile; (b) vertical gas gun; (c) protection cage; (d) clamping device; (e) rubber ‘rebound catcher’.

The impact velocity of the projectile can be varied by adjusting the chamber pressure of air that operates the gas gun. The relationship between the impact velocity and the chamber pressure was calibrated before conducting the impact tests with the sandwich panels. A pair of Omron E32 fibre optic sensors were positioned 100 mm apart, along the path of flight of the projectile to measure the initial impact velocity. The velocity counters were not used

during the actual test in order to prevent accidental damage from the projectile. Fig. 2 shows the calibration results based on ten different pressures from 0.1 to 0.6 MPa, and there were three shots carried out for each pressure. It is clear that the relationship between the impact velocity and air pressure approximately follows a second-order polynomial.

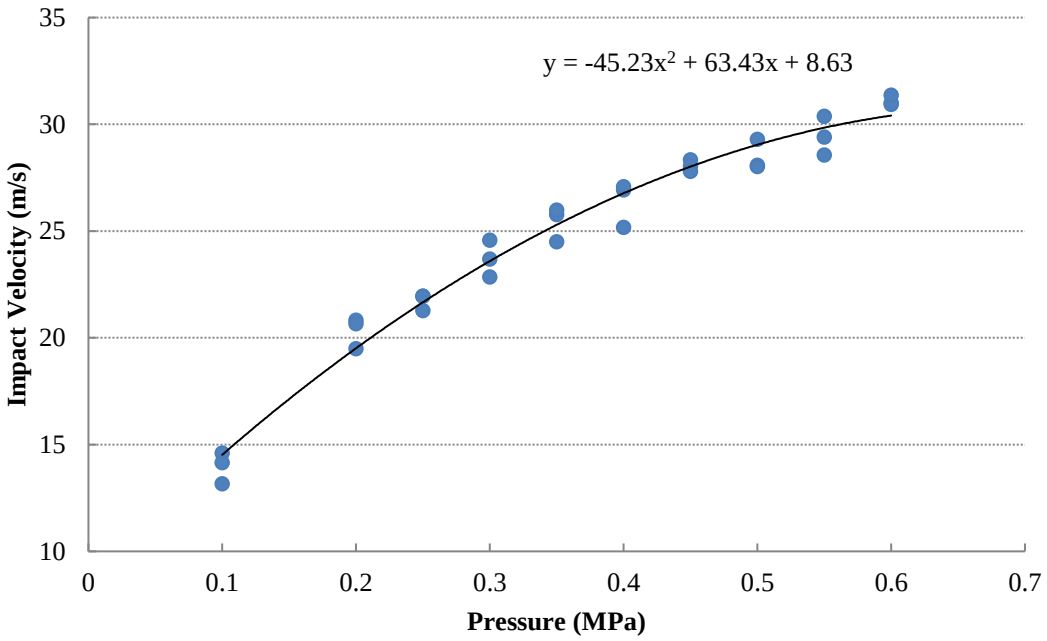

Fig. 2. Calibration of the relationship between impact velocity and chamber pressure.

A high speed digital camera (Redlake MotionPro X3) was used to record the impact process at a sampling rate of 5000 fps. Fig. 3 shows the selected high speed video frames displaying the process of 43 J impact on PS foam core sandwich panel. A datum point was painted on the projectile for tracking using image analysis software. The velocities of projectile just before and after impact were determined from the high speed camera images. Since there was some scatter in the calibration plots shown in Fig. 2, the initial impact velocity measured from the high speed camera pictures was used to calculate the initial kinetic energy for each test.

The data recorded from accelerometer and high speed camera were used to plot the contact force–time and force–displacement curves. The energy absorbed by the different sandwich panels, calculated from the area under the force–displacement curves, was compared. After the test, the deformations of the front and back facesheets were measured by 3D scanning technique; the overall bending deflection and local indentation depth on the front and back faces were quantitatively compared. Finally, the tested panels were cut transversely through the impact centre and the cross sections were examined to investigate the internal damage to the sandwich panels.

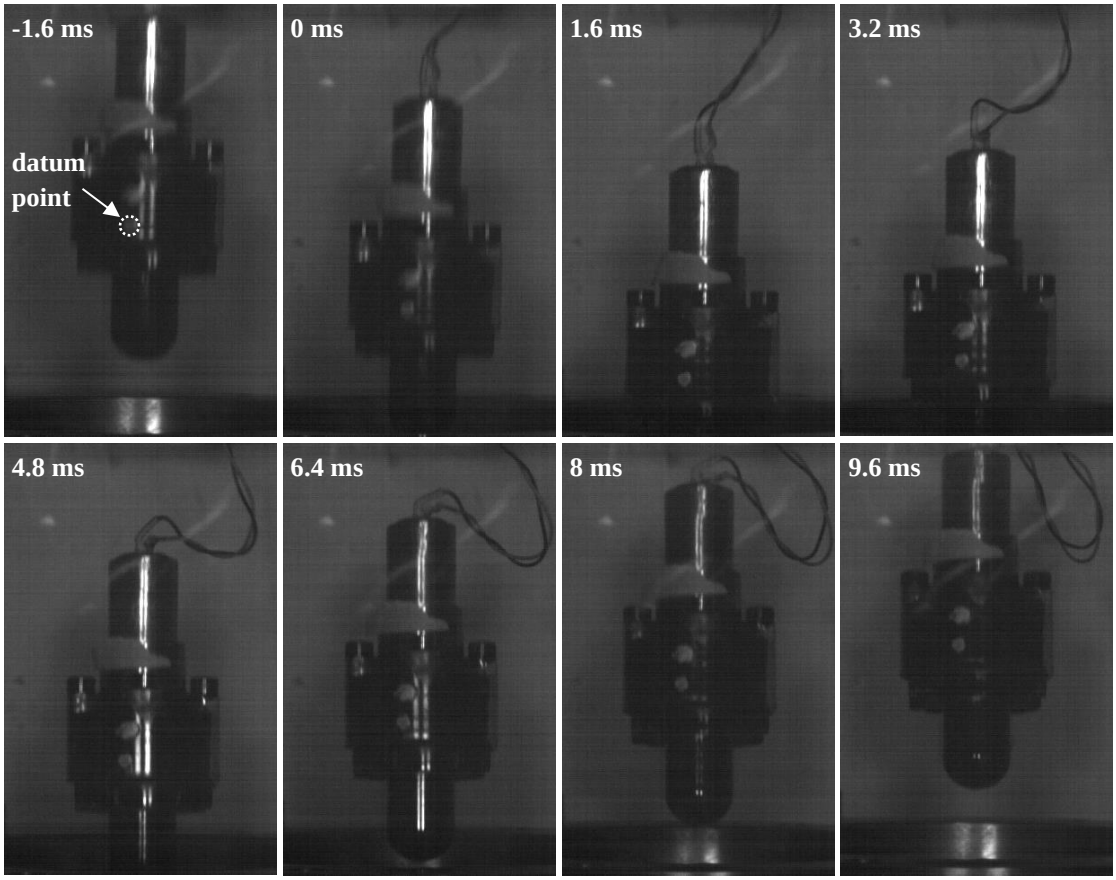

Fig. 3. Selected high-speed video frames showing the process of 43 J impact on PS foam core sandwich panel.

3. Results and discussion

3.1. Sensor measurements

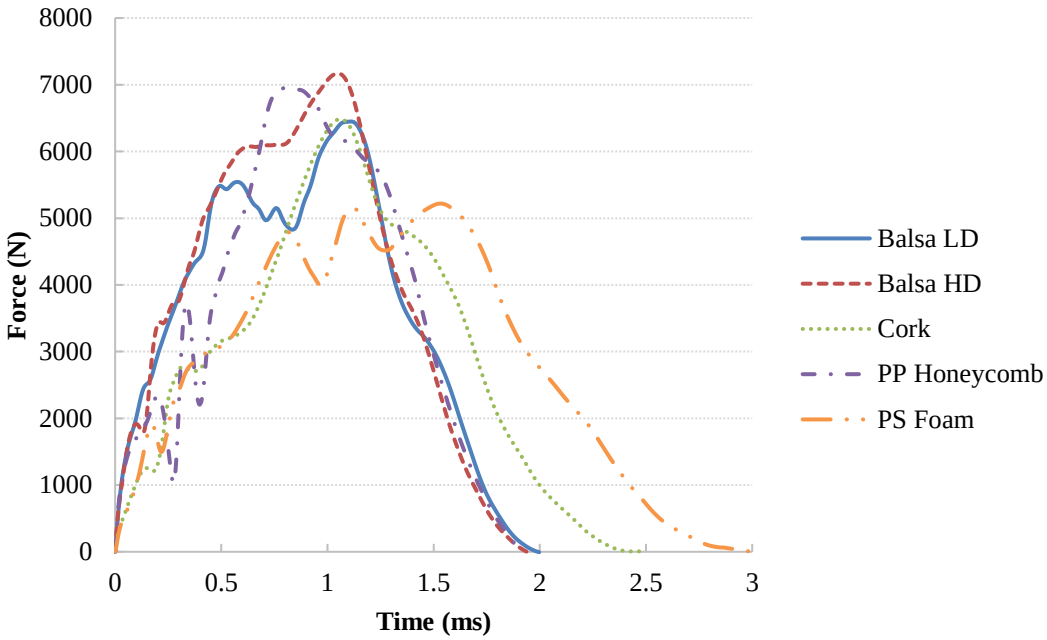

Fig. 4. Contact force histories of 43 J impact on sandwich panels.

The force history of every test was plotted to analyse how the contact force changed with time. The peak force and impact duration were determined as well. Fig. 4 shows the contact force histories of sandwich panels subjected to impact energy of 43 J. It can be seen that the force histories of all the sandwich panels irrespective of the core material show the same tendency, namely, the force history curve exhibiting an almost linear increase as the projectile contacts the panel and is followed by a prolonged contact with the core. There is a sudden drop in the force after it reaches the first peak value, which indicates a loss of stiffness caused by debonding or crack in the core. In some cases, the densification of core material causes the force to rise again after the initial drop. The sandwich panel is unloaded after the maximum force value is reached. It should be mentioned that there is oscillation existing in the force histories which is caused by the elastic wave propagation in the

sandwich panel and projectile. So the magnitudes of the measured peak forces are only accurate to a certain extent.

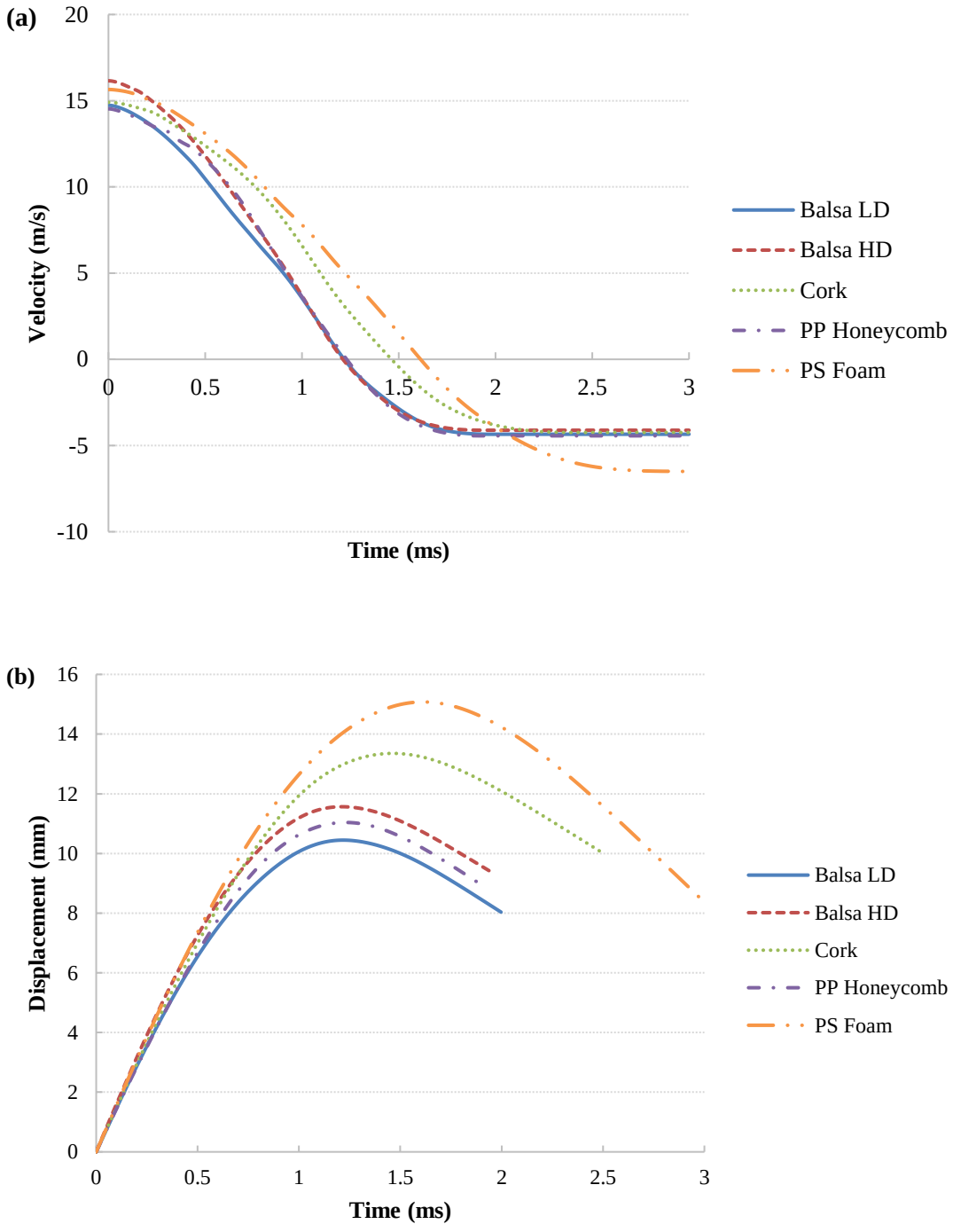

Fig. 5. (a) Velocity histories and (b) displacement histories of 43 J impact on sandwich panels.

Fig. 5 shows the velocity and displacement histories of the projectile during the 43 J impact on the sandwich panels. The velocity history of projectile was calculated from integrating the acceleration data and using the initial impact velocity obtained from the high speed camera. Subsequently, the corresponding displacement history of the projectile was then calculated from integrating the velocity.

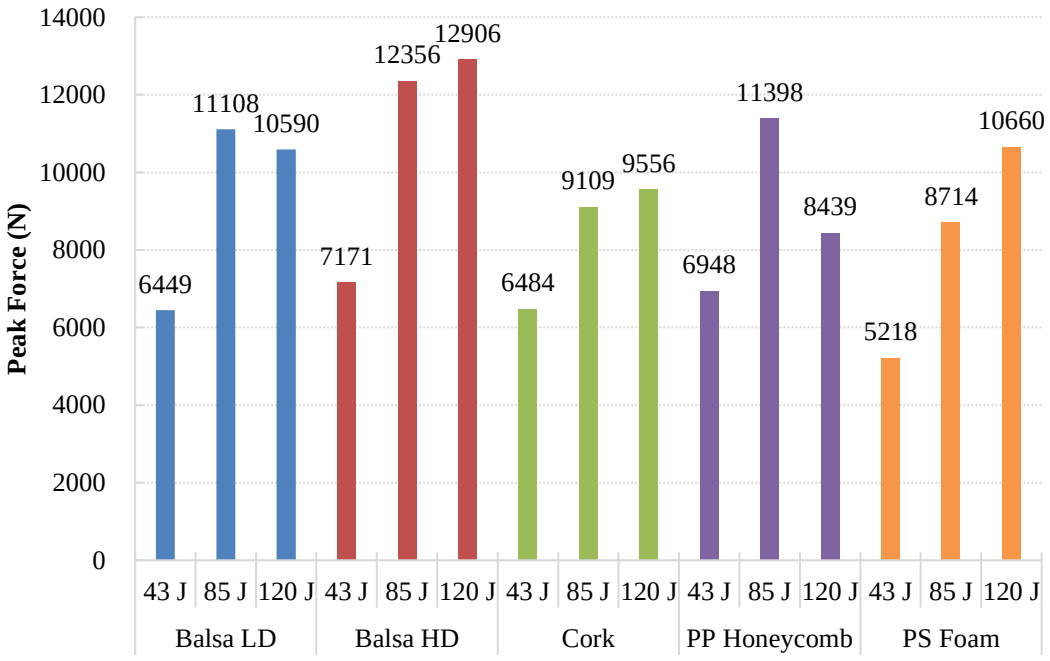

Fig. 6. Peak force of sandwich panels subjected to different impact energies.

The peak contact force of all the sandwich panels subjected to different impact energies are summarised in Fig. 6. It is clear that the peak force of sandwich panel with Balsa HD core is the highest among the five panels for all the three impact energies. When the impact energy is increased from 43 to 85 J, the peak forces dramatically increase for all the five panels. However, when the impact energy is further increased to 120 J, the peak force keeps almost constant for sandwich panels with Balsa LD, Balsa HD, and Cork cores. This suggests a critical peak force for particular sandwich configuration. It is interesting that the peak force drops from 11398 to 8439 N for PP honeycomb core panel, which may be caused by the non-

uniformity of honeycomb structure at different locations. The PP honeycomb has a cell size of 8 mm; it is possible that the response to an impact at the centre of a cell will be slightly different from that at an intersection of walls. However, the influence of this detail was not examined.

3.2. Force–displacement curves of sandwich panels

The force and displacement histories are combined to obtain the force–displacement curves of the medium velocity impact on the sandwich panels. The force–displacement curves of projectile for 43, 85, and 120 J impact are shown in Fig. 7, Fig. 8, and Fig. 9 respectively. It is observed that all the force–displacement curves exhibit a quasi-linear behaviour for low values of displacement, followed by a non-linear regime. It is clear from the force–displacement curves that the stiffness of sandwich panel, i.e. the slope of initial linear portion of the curve, is different among the panels with different core materials, implying that the behaviour of sandwich panel is dependent on the core properties even for low values of displacement. The stiffness of sandwich panels with Balsa LD, Balsa HD, and PP honeycomb cores are higher than that of Cork and PS foam core panels. The behaviour of sandwich panel after yield exhibits a core-dominant behaviour and follows regions of plastic plateau and densification of the core. It can be seen from the force–displacement curves that the sandwich panels with core material of Balsa LD, Balsa HD, Cork, and PS foam show three distinct regions: linear part, plateau and densification. The prolonged plateau region indicates the interaction of projectile through the core.

At higher impact energy of 120 J, the core material is compressed and densified and the back facesheet begins to carry more load, a secondary peak value is observed. The different force–displacement behaviour of PP honeycomb core sandwich panel is caused by the damage in

honeycomb consists of the buckling of cell walls, while the damage in other cores is in the form of crushing and cracking.

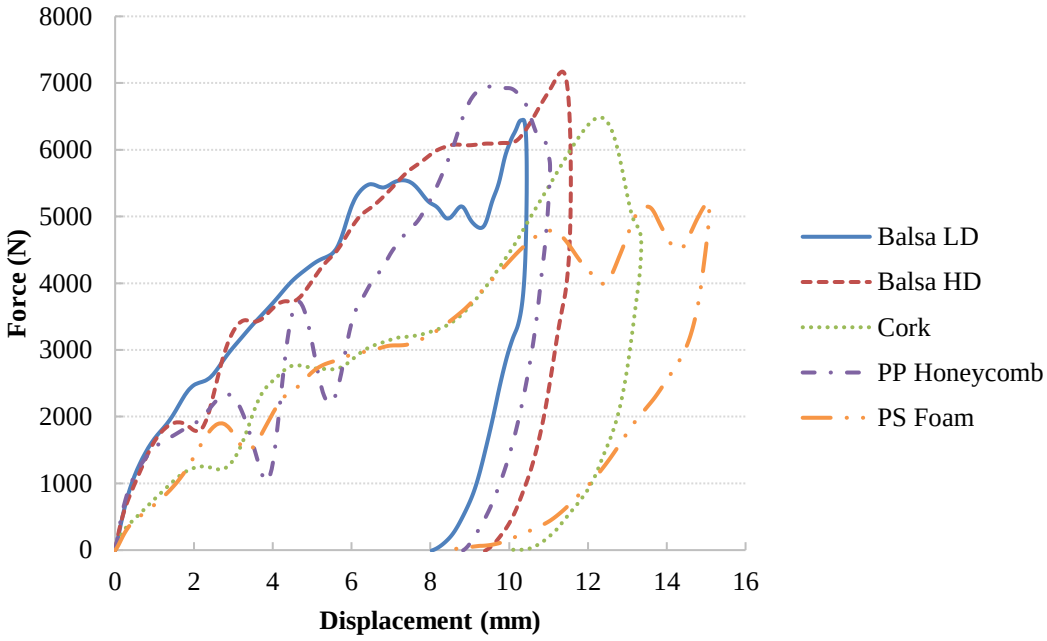

Fig. 7. Force–displacement curves of 43 J impact on sandwich panels.

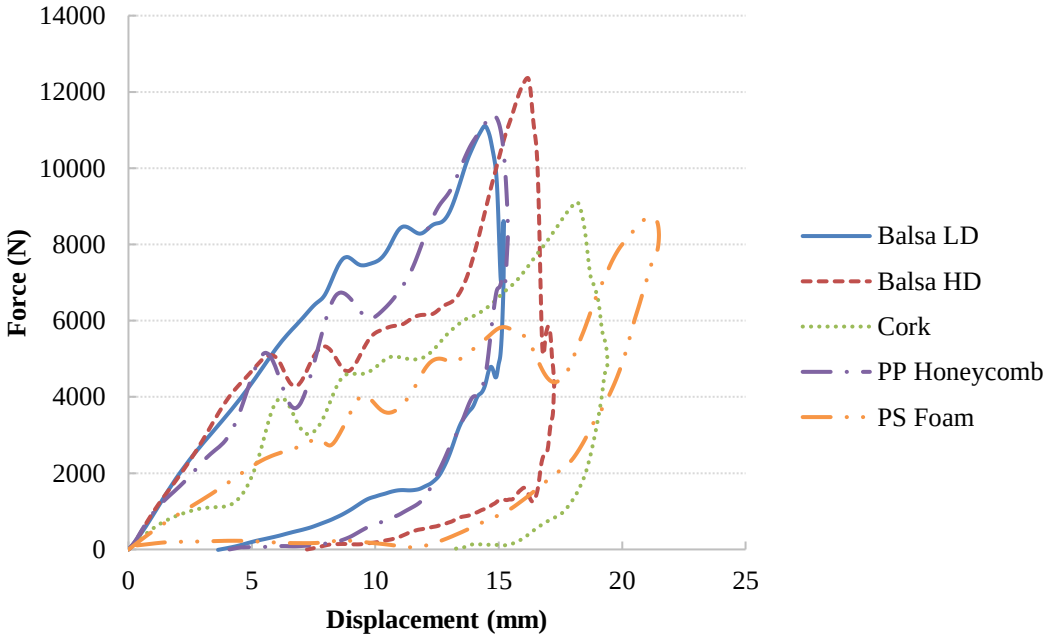

Fig. 8. Force–displacement curves of 85 J impact on sandwich panels.

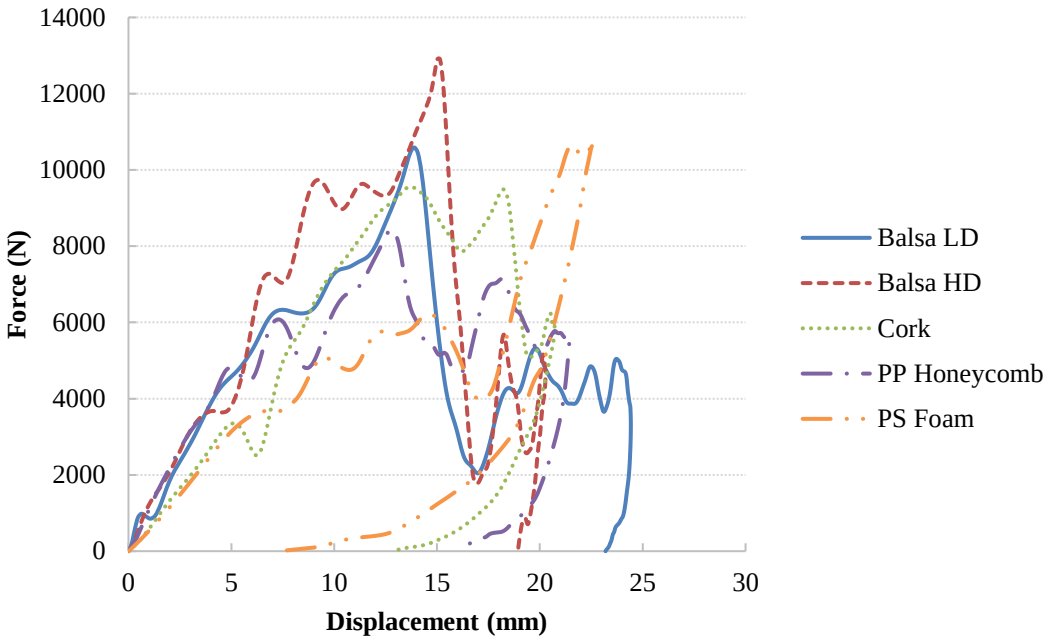

Fig. 9. Force–displacement curves of 120 J impact on sandwich panels.

3.3. Energy absorption

The energy dissipated during the impact process can be calculated from the force–displacement curve. The area enveloped by the closed curve is deemed as the absorbed energy of the sandwich panel under the specific impact and was found by numerical integration. If the impact energy is high enough, perforation will take place but this paper is limited to non-perforated impact events. The energy absorption is normalised by the total weight of the sandwich panel to take into account the different densities of the core materials. Fig. 10 summarises the specific energy absorption of sandwich panels during impact and it is clear that the absorbed energy increases with the impact energy for all the sandwich panels. This is in agreement with the observations on high velocity impact response of sandwich structures made of GFRP facesheets and polyurethane foams [24] and high velocity impact behaviour of metallic sandwich panels with aluminium foam core [16]. However, it was found that the energy absorption decreased as the impact load increased in the low velocity

impact tests on sandwich panels made of woven natural silk/epoxy composite facesheet and three different core materials [21], which is contrary to the trend observed here. The absorbed energy is a combination of energy for the plastic yielding and perforation of the facesheet as well as the crushing and failure processes in the core. The Balsa HD core sandwich panel absorbs the largest amount of specific energy among the five panels at impact energies of 43 and 85 J, however, Balsa LD core specimen outperforms the higher density balsa at 120 J impact. The lightest sandwich panel with PS foam core absorbs the least energy of 74.3 J for an impact of 120 J and the performance is not improved even if we consider the specific energy value.

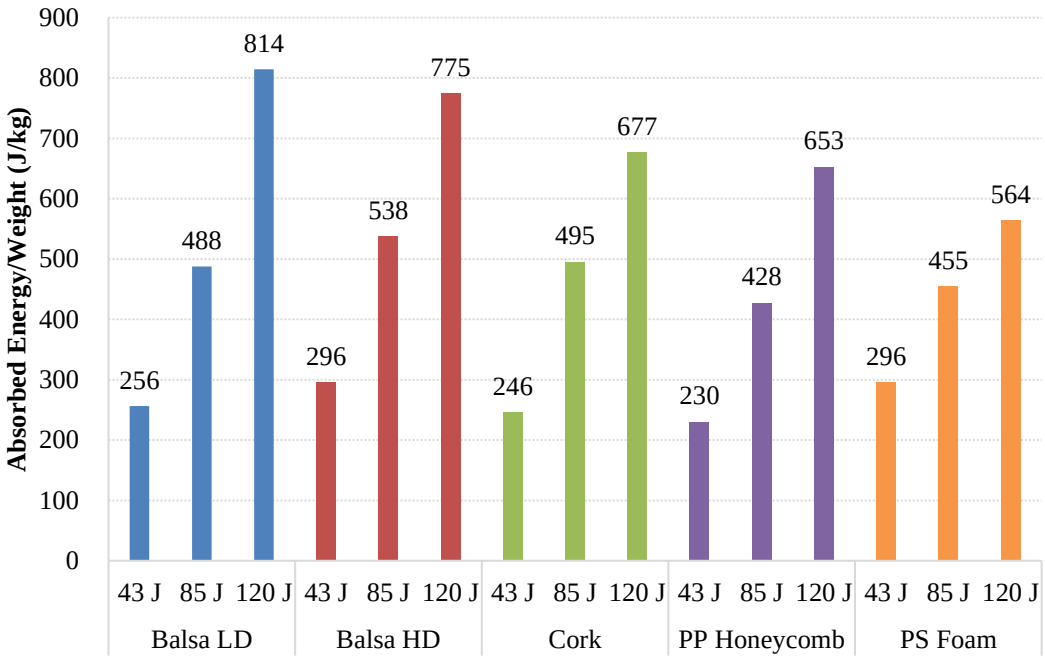

Fig. 10. Specific energy absorption of sandwich panels subjected to different impact energies.

3.4. Depth map of deformation

The impact induced residual deformation of the sandwich panel includes the overall bending deflection and local indentation around the impact centre, as shown in Fig. 11 (a). The maximum residual deformation including the global bending and local indentation

components on the front and back facesheets, as shown in Fig. 11 (b) and (c) respectively, are measured from the 3D scan of the tested sandwich samples. The total deformation, global bending deflection, and local indentation all have an increasing trend with impact energy on both of the faces. On the front facesheet, local indentation is the main component for sandwich panels with Balsa LD, Balsa HD, and PP honeycomb cores which have higher Young's moduli compared to Cork and PS foam. The sandwich panel with the PP honeycomb core has the least overall bending deformations, which could be attributed to the PP honeycomb having the highest Young's modulus of all the cores; however, its local deformation, especially on the front surface is quite high, indicating considerable core damage. For the sandwich panels with Cork core, except at the lowest impact energy, the local indentation of the top surface is lower than its global bending deformation. The top face local deformation is the least (and the bending deformation the highest) for sandwich panel with the PS foam core. It is also noteworthy that as the input energy increases from 43 to 120 J, the increase in local deformation of the top face of the PS core panel is quite small from 2.15 to 2.33 mm (unlike the other sandwich panels), while the global bending deformation increases by 150%. The relative magnitudes of the local indentation and global bending deformations of the back face of the PS foam core sandwich panel are similar to those of the front facesheet. On the other hand, in the majority of the other samples, especially the sandwich panel with the Balsa HD core, the deformation is more locally defined, both on the front as well as the rear facesheets. For Balsa LD core sandwich panel subjected to 120 J impact, the local indentation accounts for 40% of the total deformation on the back face, this is because the back facesheet was ruptured (see Section 3.5).

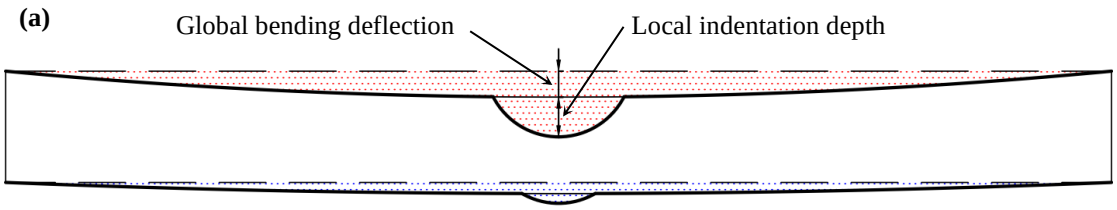
(a)
Global bending deflection
Local indentation depth

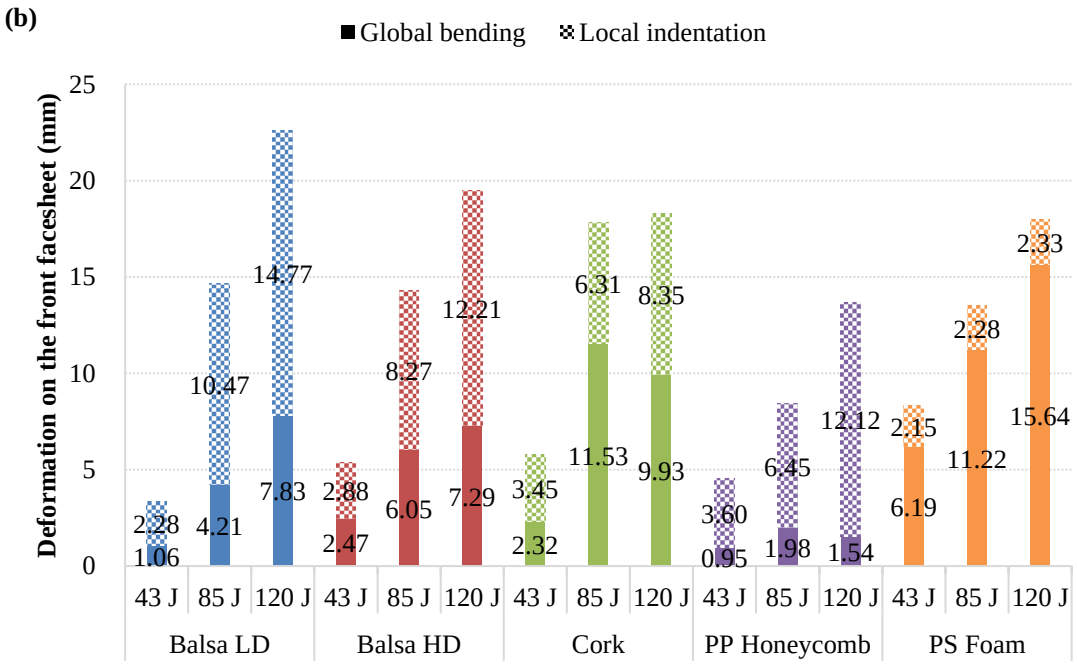
(b)
Global bending
Local indentation
Deformation on the front facesheet (mm)
25
20
15
10
5
0
2.28
1.06
4.21
10.47
7.83
14.77
2.88
2.47
6.05
8.27
7.29
12.21
3.45
2.32
11.53
6.31
9.93
8.35
3.60
0.95
1.98
6.45
1.54
12.12
2.15
6.19
11.22
2.28
15.64
2.33
43 J
85 J
120 J
Balsa LD
Balsa HD
Cork
PP Honeycomb
PS Foam

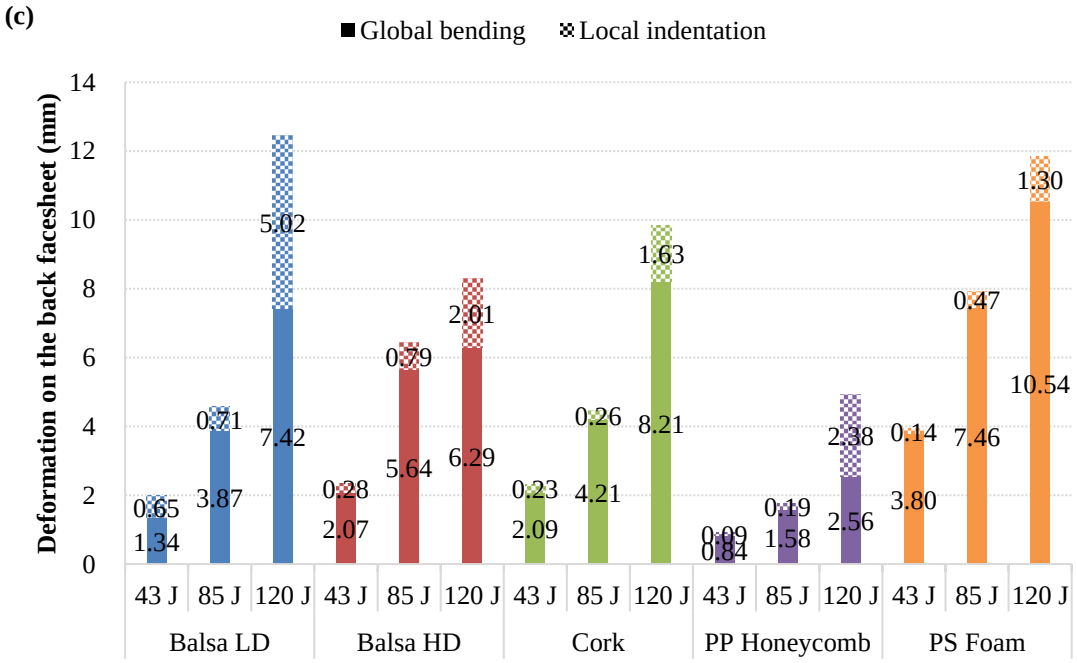
(c)
Global bending
Local indentation
Deformation on the back facesheet (mm)
14
12
10
8
6
4
2
0
0.65
1.34
3.87
0.71
7.42
5.02
0.28
2.07
5.64
0.79
6.29
2.01
0.23
2.09
4.21
0.26
8.21
1.63
0.09
0.84
1.58
0.19
2.56
2.38
0.14
3.80
7.46
0.47
10.54
1.30
43 J
85 J
120 J
Balsa LD
Balsa HD
Cork
PP Honeycomb
PS Foam

Fig. 11. (a) Schematic diagram of the deformation of sandwich panel, (b) total deformation on the front facesheet, and (c) total deformation on the back facesheet.

The depth map of total deformation for both the front and back facesheets of all the sandwich panels subjected to impact of 120 J is given in Fig. 12. It is found that the sandwich panels with Balsa LD, Balsa HD, and PP honeycomb cores which have high stiffness show circular depth map on the front facesheet. However, the depth map of Cork and PS foam core sandwich panels exhibit a rhombus shape on the front facesheet, which suggests that the sandwich panel undergoes large deformation that the clamping force was different between corners and sides of the sample. This has a huge effect on the distortion of the panels with low stiffness. In hindsight, this clamp was not ideal for medium velocity impact as the square samples of 150 mm × 150 mm were clamped in circular ring with internal diameter of 135 mm. Also, it is clear that the sandwich panel with PP honeycomb core has the smallest deformation both on the front and back facesheets. It is even almost undeformed in the area outside the impact location on both the front and back facesheets.

Fig. 13 shows the depth map of deformation on the front facesheet for sandwich panels with Balsa HD and PS foam cores at the different energies of impact. The two core materials were chosen to illustrate the two different behaviours of highly local and global deformation of the sandwich panel, respectively. It can be seen that the deformations increase as the impact energy increases for both types of sandwich panels.

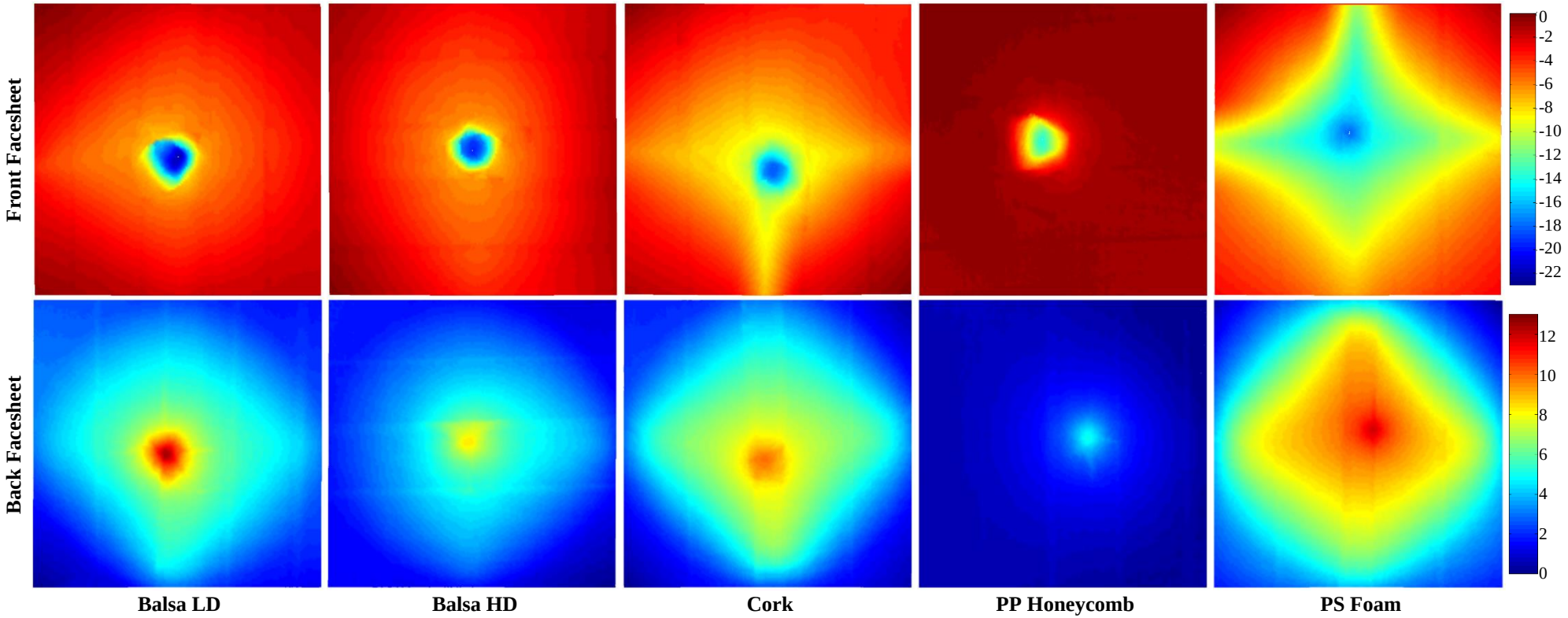

Fig. 12. Depth map of deformation on both the front and back facesheets of sandwich panels with different cores subjected to 120 J impact (unit: mm).

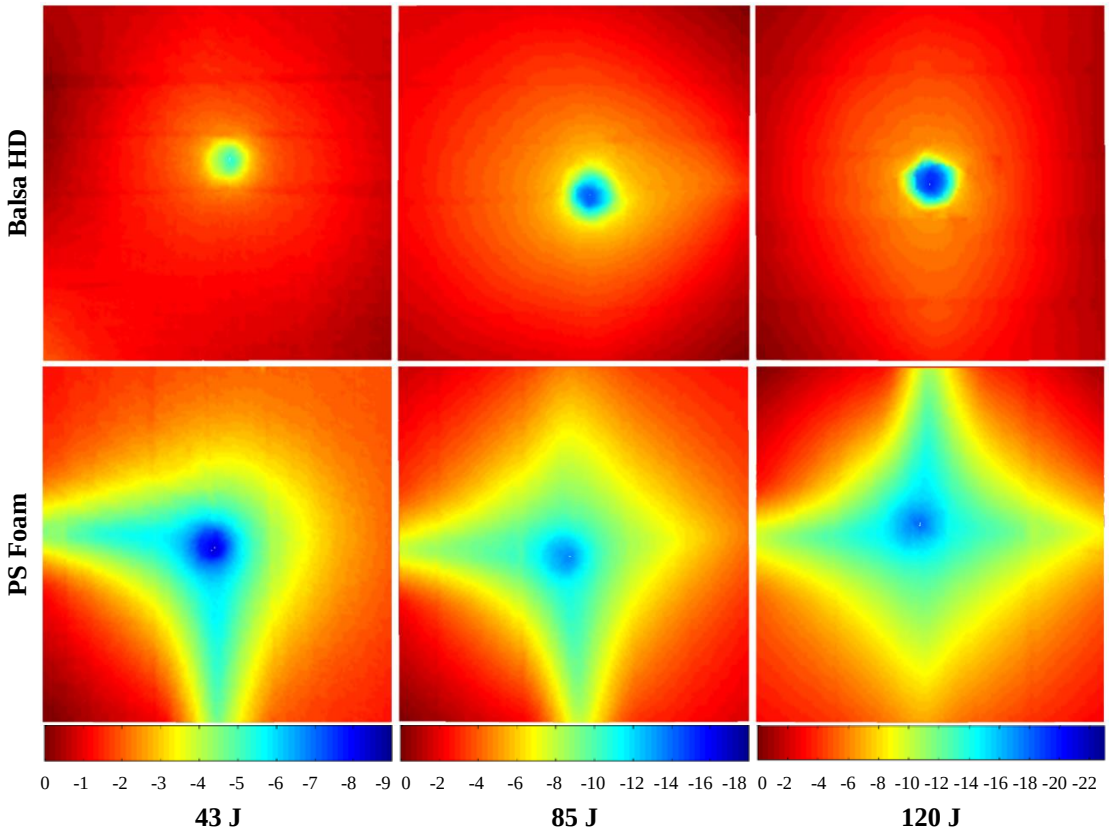

Fig. 13. Depth map of deformation on the front facesheet of sandwich panels with Balsa HD and PS foam cores subjected to different impact energies (unit: mm).

3.5. Post-mortem damage analysis

The tested sandwich panels were cut carefully through the impact point, and the cross section views of the panels after 120 J impact are presented in Fig. 14. It can be seen that the impact induced damage modes include facesheet rupture, core crushing, and debonding between facesheet and core. Table 2 summarises the damage modes induced by the 120 J impact on sandwich panels with different cores. 'Y' means the corresponding damage mode occurs in the specimen, while 'N' denotes the absence of visible signs of that damage mode. It is to be noted that while the front facesheet has ruptured in every other case, for the sandwich panel with the PS foam core, neither the front nor the rear facesheet has ruptured, there is no debonding of the facesheets and the core crushing, if any is minimal. It is clear that local damage is minimal for

sandwich panel with PS foam core even under impacts of 120 J, which leads to the inference that the PS core would offer the most resistance against projectile penetration, even at higher energies.

The front facesheets of all the sandwich panels except the PS foam core sandwich were perforated after 120 J impact. Kolopp et al. [4] found the front facesheet choice was very important for the target penetration resistance, and Abrate [34] also noted that the penetration resistance was strongly influenced by the facesheets. The facesheets used here are identical for all the sandwich panels, but a difference in penetration resistance is observed. This shows that the core material plays an important role in impact resistance and that other factors such as overall rigidity of the sandwich are also important. The sandwich panels with higher overall rigidity, like Balsa HD and PP honeycomb core specimens, have bigger local indentation but smaller overall bending deflection. The sandwich panels with lower rigidity present the opposite case. Balsa LD core panel is the only sandwich that shows the beginning of rupture in the back facesheet. The aluminium facesheets generally fail through plug initiation and the formation of petals, which is a typical damage mode of ductile plates [35]. The lower elastic modulus and the greater foundational support provided by the PS foam core has facilitated energy absorption mainly through global bending of the sandwich panel without local rupture of the facesheet. While such a magnitude of overall bending may not be desirable in all cases, it would appear that if resistance to local penetration is the key objective, then the PS foam would be the material of choice among all the different cores studied here. This study focuses on the impact without complete perforation of the sandwich panels, so the effect of core material on the perforation threshold cannot be established here.

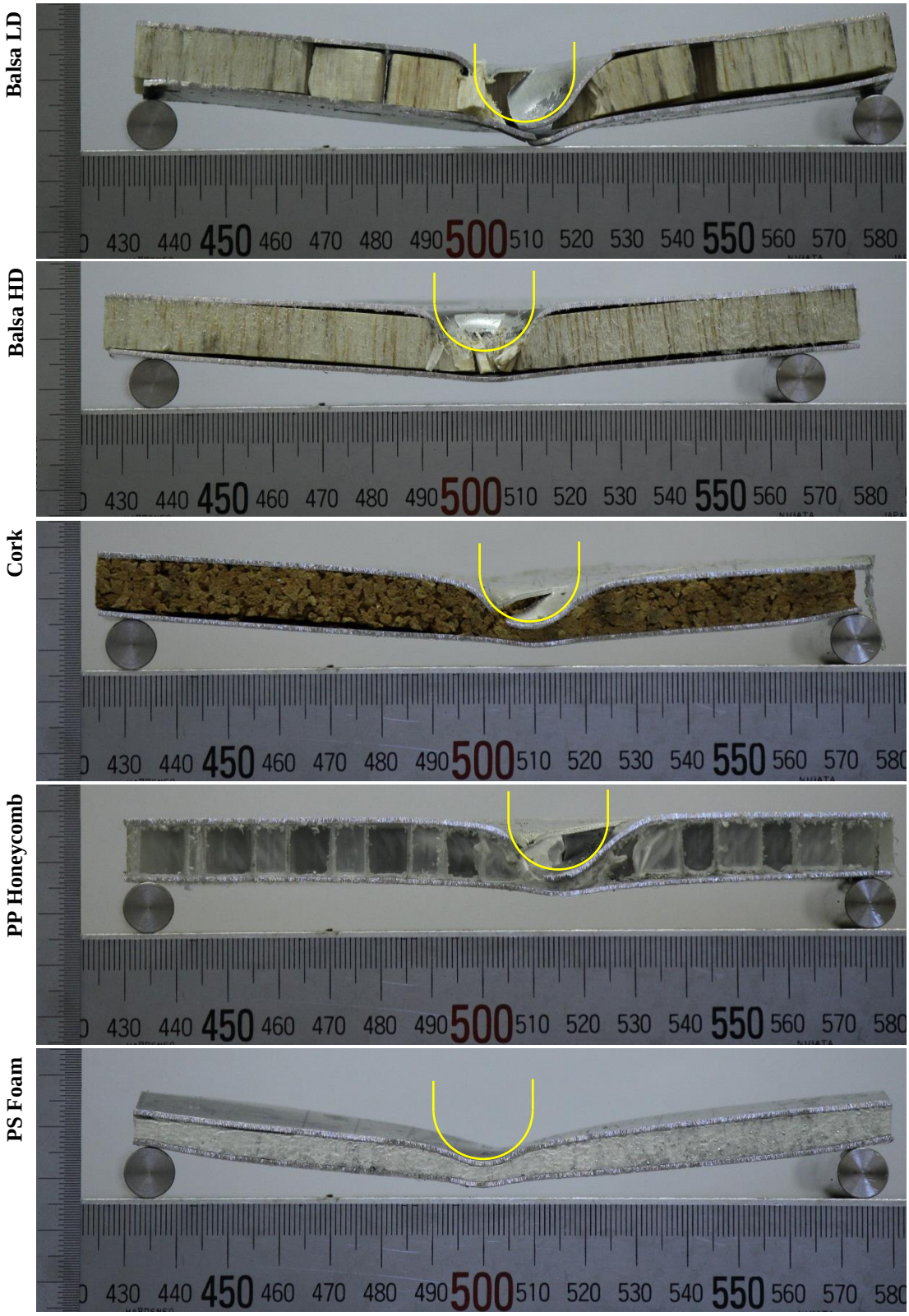

Fig. 14. Cross section views of sandwich panels after 120 J impact.

Table 2. Summary of damage mechanisms induced by 120 J impact on sandwich panels.

Damage Mechanisms	Facesheet Rupture		Core Crushing	Debonding	
	Front	Back		Front	Back
Balsa LD	Y	Y	Y	Y	Y
Balsa HD	Y	N	Y	Y	Y
Cork	Y	N	Y	N	Y
PP Honeycomb	Y	N	Y	N	N
PS Foam	N	N	N	N	N

The deformation and damage in the core material is also visible in the Fig. 14. The occurrence of core crushing in the sandwich panels at a point immediately beneath the impact is consistent with that of front facesheet rupture, i.e., the impactor is in direct contact with the core after the rupture of the front facesheet. Interface debonding between the facesheet and core material was observed in the sandwich panels with Balsa LD, Balsa HD, and Cork cores. Additionally, Balsa LD core was even broken into pieces after 120 J impact. This suggests that there is radial crack propagation from the impact point to the periphery observed in the Balsa cores of both densities due to the brittleness of the balsa wood. Fig. 15 shows the Balsa HD core material after 120 J impact. A splintering failure at the point of impact followed by a radial cracking is evident for the wood core. The broken pieces of Balsa LD core is due to the combination of conical and radial cracks which is typical of brittle material failure.

Fig. 15. Radial crack propagation from the impact point to the vicinity of Balsa HD core subjected to 120 J impact.

It is also noted that the rigid core materials will constrain the out-of-plane deflection of the front facesheet and confine it to high local indentation which lead to front facesheet rupture and core crushing at the impact point, while soft core materials like PS foam allow the sandwich to bend globally over a larger area. It is observed that the residual deformation of the PS foam core specimen reaches the plate boundary, and the foam core becomes thinner after impact. On the contrary, the PP honeycomb core specimen is almost not deformed in the regions outside of the impact location.

From the Figs. 10 and 14, it is possible to correlate the severity of damage to the energy absorption, i.e., the sandwich panel which suffers more damage absorbs more energy during the impact. Buitrago et al. [36] identified that the facesheets were the main factor responsible for the energy absorption at high velocity impact, noting that the front facesheet and the back facesheet accounted for 46% and 41% of the absorbed energy respectively, while the core was responsible for merely 13% at 287

m/s impact in their study. This is true for sandwich samples with rigid cores that exhibit mainly local deflection. We can observe that facesheet rupture is associated with significant energy absorption in the sandwich panels with front facesheet perforation. However, for medium velocity impacts in the case of flexible core sandwich panels, the energy was mainly absorbed by the large plastic deformation of the facesheets that extended from the impact location to the boundary. Therefore it is clear from the results of this study that even when the core is not the main energy absorbing component, it greatly influences the energy absorption, damage mechanisms, and penetration resistance of the sandwich panel for medium velocity impacts.

It is also clear from Fig. 14 that the sandwich panel with PS foam core has the least overall material damage, which indicates that the sandwich panel with the PS foam core will be able to absorb higher levels of energy (than we have tested) before it has penetration and starts failing. As can be seen from Fig. 6, the peak forces for corresponding energy levels are lower in the sandwich panel with PS foam than the other panels, which means that the local strains and stresses will be lower; hence the margin of safety for material failure higher. In the case of the other panels, if the impact energy is raised above 120 J soon they will suffer complete penetration of both front and rear surfaces and hence the energy absorbed will plateau; whereas, in the case of the sandwich panel with PS foam, complete penetration and plateauing will occur only at a much higher impact energy. Hence it can be concluded that the sandwich panel with the PS foam core will have the highest energy absorption before failure of all the panels tested. This may be attributed to (a) the lower overall bending stiffness of the panel with PS foam core, and (b) the fact that the PS foam appears to provide much greater foundational elastic support to the sandwich skins, allowing the

deformation to spread throughout the entire panel much more evenly and allowing the skins to absorb a much greater fraction of energy through overall bending. So it appears that the sandwich panel with the PS foam would be the most suitable among those tested for applications in which we want resistance to penetration or higher energy absorption before failure.

It can be seen from Fig. 10 that the increase in energy absorbed per unit weight is the least for the PS foam core sandwich, increasing less than 100% (from 296 to 564 J/kg) when the input impact energy nearly triples from 43 to 120 J. The peak of the force-displacement curves indicate the point at which either projectile loses contact with the target (rebouncing) or the target suffers damage sufficient to reduce its resistance to impact. Thus the energy denoted by the area of the force-displacement curve up to the peak point is a key indicator of the energy absorption characteristic of panel before begins to fail. Fig. 16 shows the fraction of energy absorbed by each panel (strain energy up to the peak of the force-displacement curve divided by input energy). It can be seen that in all cases, except those of the panels with the Balsa HD and the PS foam cores, there is a significant drop at the impact of 120 J, indicating considerable rupture and failure of the panel and reduction in its load carrying capacity. In the case of sandwich panel with Balsa HD core, the energy fraction drops by 6% and 16% as the input energy increases from 43 to 85 and 120 J. In the case of the panel with PS foam core, reduction in energy fraction is under 10% when the input energy is increased to 120 J, indicating that it is quite capable of withstanding higher energy impacts. This is also supported by the absence of any significant damage observed in the post-mortem analysis.

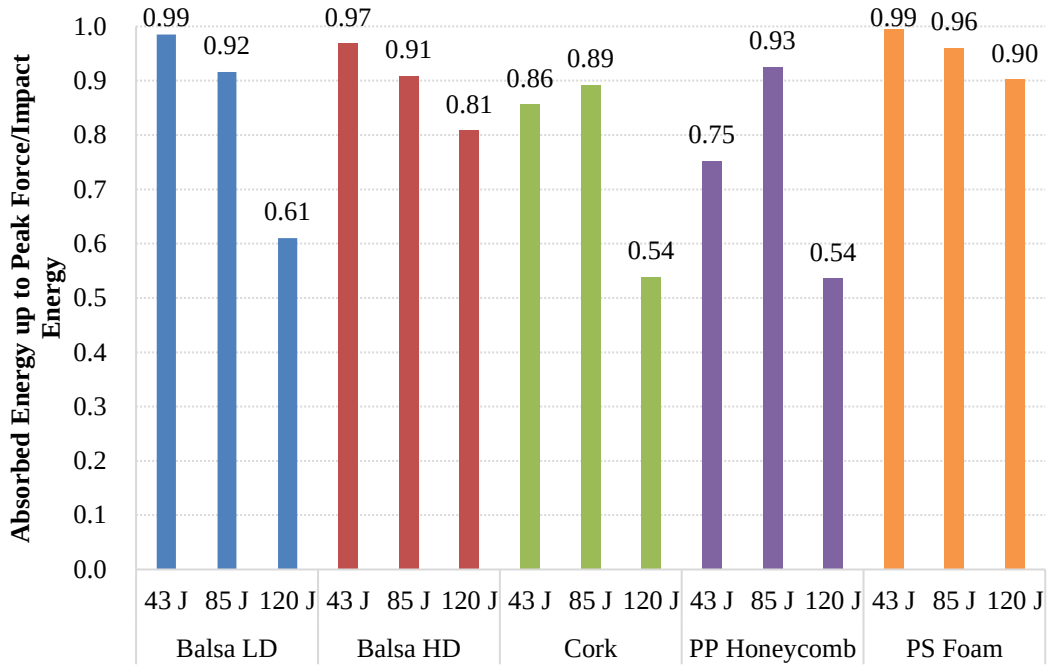

Fig. 16. Fraction of energy absorbed up to peak force.

4. Conclusions

This paper experimentally investigates the influence of core material on the response of sandwich structures subjected to medium velocity impact. Impact tests were conducted on sandwich panels with five different core materials using an instrumented gas gun. The sandwich panels were compared in terms of their force-displacement curves, specific energy absorbed and damage mechanisms. The core material is found to be very important in the target deformation, energy absorption, damage mechanisms, and penetration resistance of the sandwich panel. Based on actual application requirements, the performance can be optimized with the proper choice of core material. If the primary design parameter is energy absorption and penetration resistance, Polystyrene foam is a promising core material but this requires further investigation. Polypropylene honeycomb is the optimal choice for core if

minimal back face deformation is chosen as the performance criterion. The impact test results and the damage analysis of the sandwich panels provide the designer with some insight about the sandwich panels with different core materials. A combination of the experimental data presented in this paper and simulation results of the sandwich panels using finite element models will be an invaluable tool to the designer in choosing the appropriate material for their application.

References

[1] Mackerle J. Finite element analyses of sandwich structures: a bibliography (1980–2001). Engineering Computations. 2002;19:206-45.

[2] Ramakrishnan KR, Guérard S, Viot P, Shankar K. Effect of block copolymer nano-reinforcements on the low velocity impact response of sandwich structures. Composite Structures. 2014;110:174-82.

[3] Chai GB, Zhu S. A review of low-velocity impact on sandwich structures. Proceedings of the Institution of Mechanical Engineers, Part L: Journal of Materials Design and Applications. 2011;225:207-30.

[4] Kolopp A, Rivallant S, Bouvet C. Experimental study of sandwich structures as armour against medium-velocity impacts. International Journal of Impact Engineering. 2013;61:24-35.

[5] Cantwell W, Dirat C, Davies P. A comparative study of the mechanical properties of sandwich materials for nautical construction. SAMPE Journal(USA). 1994;30:45-51.

[6] Park JH, Ha SK, Kang KW, Kim CW, Kim HS. Impact damage resistance of sandwich structure subjected to low velocity impact. Journal of Materials Processing Technology. 2008;201:425-30.

[7] Ozdemir O, Karakuzu R, Al-Shamary AKJ. Core-thickness effect on the impact response of sandwich composites with poly(vinyl chloride) and poly(ethylene terephthalate) foam cores. J Compos Mater. 2015;49:1315-29.

[8] Shipsha A. Failure of sandwich structures with sub-interface damage: Royal Institute of Technology, Stockholm; 2001.

[9] Li QM, Mines RAW, Birch RS. The crush behaviour of Rohacell-51WF structural foam. International Journal of Solids and Structures. 2000;37:6321-41.

[10] Bhuiyan MA, Hosur MV, Jeelani S. Low-velocity impact response of sandwich composites with nanophased foam core and biaxial braided face sheets. Composites Part B: Engineering. 2009;40:561-71.

[11] Vinson JR. Sandwich Structures. Applied Mechanics Reviews. 2001;54:201-14.

[12] Bernard ML, Lagace PA. Impact resistance of composite sandwich plates. Journal of Reinforced Plastics and Composites. 1989;8:432-45.

[13] Atas C, Sevim C. On the impact response of sandwich composites with cores of balsa wood and PVC foam. Composite Structures. 2010;93:40-8.

[14] Mohan K, Yip TH, Idapalapati S, Chen Z. Impact response of aluminum foam core sandwich structures. Materials Science and Engineering: A. 2011;529:94-101.

[15] Rajaneesh A, Sridhar I, Rajendran S. Relative performance of metal and polymeric foam sandwich plates under low velocity impact. International Journal of Impact Engineering. 2014;65:126-36.
[16] Hou W, Zhu F, Lu G, Fang D-N. Ballistic impact experiments of metallic sandwich panels with aluminium foam core. International Journal of Impact Engineering. 2010;37:1045-55.
[17] Abrate S. Impact on laminated composite materials. Applied Mechanics Reviews. 1991;44:155-90.
[18] Cantwell W, Morton J. The impact resistance of composite materials—a review. Composites. 1991;22:347-62.
[19] Vaidya U. Impact Response of Laminated and Sandwich Composites. In: Abrate S, editor. Impact Engineering of Composite Structures: Springer Vienna; 2011. p. 97-191.
[20] Zhou J, Hassan MZ, Guan Z, Cantwell WJ. The low velocity impact response of foam-based sandwich panels. Composites Science and Technology. 2012;72:1781-90.
[21] Ude AU, Ariffin AK, Azhari CH. Impact damage characteristics in reinforced woven natural silk/epoxy composite face-sheet and sandwich foam, coremat and honeycomb materials. International Journal of Impact Engineering. 2013;58:31-8.
[22] Crupi V, Kara E, Epasto G, Guglielmino E, Aykul H. Prediction model for the impact response of glass fibre reinforced aluminium foam sandwiches. International Journal of Impact Engineering. 2015;77:97-107.
[23] Wang J, Waas AM, Wang H. Experimental and numerical study on the low-velocity impact behavior of foam-core sandwich panels. Composite Structures. 2013;96:298-311.
[24] Nasirzadeh R, Sabet AR. Study of foam density variations in composite sandwich panels under high velocity impact loading. International Journal of Impact Engineering. 2014;63:129-39.
[25] Yang M, Qiao P. Higher-order impact modeling of sandwich structures with flexible core. International Journal of Solids and Structures. 2005;42:5460-90.
[26] Raju KS, Smith BL, Tomblin JS, Liew KH, Guarddon JC. Impact damage resistance and tolerance of honeycomb core sandwich panels. J Compos Mater. 2008;42:385-412.
[27] Bernard LA. Low velocity impact testing of sandwich panels with polymeric cores [Honours Thesis]. Canberra: University of New South Wales at the Australian Defence Force Academy; 2011.
[28] Chalk C. Damping of sandwich panels [Honours Thesis]. Canberra: University of New South Wales at the Australian Defence Force Academy; 2011.
[29] Toson B, Viot P, Pesqué JJ. Finite element modeling of Balsa wood structures under severe loadings. Engineering Structures. 2014;70:36-52.
[30] Roach AM, Evans KE, Jones N. The penetration energy of sandwich panel elements under static and dynamic loading. Part I. Composite Structures. 1998;42:119-34.
[31] Denneulin S, Viot P, Leonardi F, Lataillade J-L. The influence of acrylate triblock copolymer embedded in matrix on composite structures' responses to low-velocity impacts. Composite Structures. 2012;94:1471-81.
[32] Tita V, de Carvalho J, Vandepitte D. Failure analysis of low velocity impact on thin composite laminates: Experimental and numerical approaches. Composite Structures. 2008;83:413-28.
[33] Sevkat E, Liaw B, Delale F, Raju BB. Drop-weight impact of plain-woven hybrid glass–graphite/toughened epoxy composites. Composites Part A: Applied Science and Manufacturing. 2009;40:1090-110.
[34] Abrate S. Localized Impact on Sandwich Structures With Laminated Facings. Applied Mechanics Reviews. 1997;50:69-82.
[35] Gupta NK, Iqbal MA, Sekhon GS. Effect of projectile nose shape, impact velocity and target thickness on deformation behavior of aluminum plates. International Journal of Solids and Structures. 2007;44:3411-39.

[36] Buitrago BL, Santiuste C, Sánchez-Sáez S, Barbero E, Navarro C. Modelling of composite sandwich structures with honeycomb core subjected to high-velocity impact. Composite Structures. 2010;92:2090-6.